Excitation intensity dependence of photoluminescence from narrow ⟨100⟩- and ⟨111⟩A-grown $In_xGa_{1-x}As$/GaAs single quantum wells

T. Sauncy and M. Holtz
Department of Physics, Texas Tech University, Lubbock, Texas 79409

O. Brafman,* D. Fekete, and Y. Finkelstein
Technion Israel Institute of Technology, Haifa, Israel

(Received 20 April 1998)

We have used excitation intensity-dependent photoluminescence (PL) spectroscopy to study strained $In_xGa_{1-x}As$/GaAs ($x \approx 0.23$) single quantum wells grown along the ⟨001⟩ and ⟨111⟩A directions. PL intensities from these two quantum-well samples exhibit a linear dependence on incident power density over the excitation intensity range examined. The linewidth of the emission from the ⟨100⟩ well is well described by band-filling effects as $I_{\rm exc}$ is increased. By careful analysis of the excitation intensity dependence of the ⟨111⟩ linewidth and the corresponding blueshift of the PL peak energy, the strain-induced piezoelectric field is estimated to be 70 kV/cm. [S0163-1829(99)00607-4]

I. INTRODUCTION

$In_xGa_{1-x}As$/GaAs strained heterostructures are interesting because of the controllable variations achievable in the electronic band structure.[1,2] These variations, the result of alloying, strain, and quantum confinement, lead to important optoelectronic device applications. Of particular interest are heterostructures in which the $In_xGa_{1-x}As$ forms a pseudomorphically strained quantum well (QW) layer in the larger band-gap GaAs barrier layers. Due to its larger lattice constant, the $In_xGa_{1-x}As$ is under uniform biaxial compressive strain, provided the layers are kept below a critical thickness.[3–6] For the single $In_xGa_{1-x}As$ QW's studied here, which are bounded by thick GaAs barrier layers, the strain is present only within the well, with the GaAs remaining strain free.[7–9] When grown along any non-[001] direction, the strain creates a polarization charge density within the strained layer.[10–14] Because the polarization charge density must terminate at the strained layer boundaries, an electric field results. This piezoelectric field has been demonstrated in an $In_xGa_{1-x}As$/GaAs QW, even with barriers as small as 150 Å.[15]

In this work, we use optical excitation intensity dependent photoluminescence (PL) spectroscopy to examine narrow ⟨111⟩- and ⟨100⟩-oriented QW's. Photoluminescence is an excellent technique for investigation of band-gap-related processes in semiconductors. PL intensity and line shape are sensitive to crystalline quality, interface abruptness, material composition, and heterolayer thickness.[16,17] PL was key in determination of the critical thickness of pseudomorphically strained layers, and has been used to gain understanding of piezoelectric field effects.[2,17–23] Here we report PL experiments aimed at understanding the band-gap emission processes and the nature of the piezoelectric field in narrow QW's. The paper is organized as follows. We begin by establishing the necessary background information and experimental details. We follow with a general discussion of the effects of excitation intensity on the spectra of ⟨100⟩ and ⟨111⟩. We then discuss the excitation intensity dependence of the peak energy and the full width at half maximum. We conclude by summarizing our results.

II. BACKGROUND

The optical and electronic properties of this QW system are influenced by alloying, strain, and quantum confinement effects. We consider these as successive perturbations, in that order, on the electronic band structure of a bulk zinc-blende crystal.[24] For growth directions for which a piezoelectric polarization is induced, the effect of the strain-induced electric field is considered as a final perturbation to the system prior to determination of the confined energy levels in the quantum well. Since the piezoelectric field effectively tilts the energy bands in the wells, calculation of the confinement is nontrivial since the standard square-well solutions are not applicable.

The band offsets for a quantum-well system are generally described in terms of fractions of the difference between the band gap of the bulk, unstrained well alloy, and the barrier material. Alloy properties are taken from prior experiments, whenever possible, and are otherwise interpolated according to Vegard's law.[24] The conduction band (CB) and valence band (VB) well edges are then shifted due to strain. This defines the depths of the wells used in the determination of confined energy levels. For the direct band gap of the bulk alloy, $In_xGa_{1-x}As$ at 77 K, we use

$$E_g(x) = 1.508\text{-}1.582x + 0.485x^2 \tag{1}$$

where x is the indium mole fraction and the respective band gaps of the binary constituents are 0.411 eV and 1.508 eV for InAs and GaAs at 77 K.[25] The CB and VB offsets are defined by

$$\Delta E_c = \frac{E_c}{E_{g,\rm GaAs} - E_g(x)} \tag{2}$$

and

 ©1999 The American Physical Society

$$\Delta E_v = \frac{E_v}{E_{g,\mathrm{GaAs}} - E_g(x)} \tag{3}$$

where E_c and E_v are the unstrained well depths and $\Delta E_c + \Delta E_v = 1$. A wide variety of band offsets are reported for the $In_xGa_{1-x}As$ system (see Ref. 18 for a summary). For our calculations, we assume $\Delta E_c : \Delta E_v = 0.75:0.25$, determined from our hydrostatic pressure measurements.[26]

The incorporation of pseudomorphic strain leads to a dramatic restructuring of both the CB and VB.[4,6] For our case, the hydrostatic strain components cause the CB Γ-point minimum to shift higher in energy, while the valence-band maximum shifts downward. Shear strain components split the light hole (LH) and heavy hole (HH) of the VB Γ-point, moving the HH level to the VB maximum for compressive strain. For the ⟨100⟩-grown system, these strain effects are described in terms of the hydrostatic and shear deformation potentials a and b. For the ⟨111⟩-grown system, the rhombohedral deformation potential d must also be included. Starting with the unstrained distribution of the band-gap difference, the effect of pseudomorphic strain on the CB and VB is then used to determine the strained well depths. The band-edge shifts are found in Ref. 4, with $\epsilon_{xx} < 0$ for compressive strain. For growth along ⟨111⟩, the strain tensor contains off-diagonal components. The strain tensor components were used as in Ref. 6 to determine in-plane strain values for the ⟨111⟩ QW.

The lowest energy transition for PL emission in the strained $In_xGa_{1-x}As$/GaAs QW system is the first confined level in the conduction band ($EC1_{\mathrm{well}}$) to the first confined heavy-hole band ($\mathrm{HH1_{well}}$),[27] which we denote as $11H$. To compute the expected transition energy for the [001]-grown well, the confinement energy is determined for the CB and VB strain-shifted wells using the Ben-Daniel-Duke single-envelope function approximation method.[28] For the calculation, the strain-shifted well depth was used.

For the ⟨111⟩-grown QW, the effect of the piezoelectric field must also be considered before confined energy levels can be determined. The internal fields can be on the order of 10^2 kV/cm, dependent upon the magnitude of psuedomorphic strain.[29] Using a bulk piezoelectric approximation, the built-in polarization field is given by[30,31]

$$P_{\mathrm{pz}} = -\left(\frac{2}{\sqrt{3}}\right)(1+\gamma)e_{14}\epsilon'_{xx}, \tag{4}$$

where

$$\gamma = \frac{C_{11} + 2C_{12} - 2C_{44} - 2(e_{14}{}^2/\kappa\epsilon_o)}{\frac{1}{2}(C_{11}+2C_{12}) + 2C_{44} + 2(e_{14}{}^2/\kappa\epsilon_o)}. \tag{5}$$

e_{14} is the piezoelectric constant, C_{ij} are the elastic constants of the alloy,[32] κ is the static dielectric constant, ϵ_o is the permeability of free space, and ϵ'_{xx} is the conventional in-plane strain tensor component for the ⟨111⟩ growth axis.[25,6] The expression for γ includes experimentally determined corrections necessary for piezoelectrically active strained crystals.[30,31] The termination of the polarization charge density at the edges of the strained layer results in an electric field along the ⟨111⟩ direction:[30,31]

$$F_{\mathrm{pz}} = -P_{\mathrm{pz}}/\kappa\epsilon_o, \tag{6}$$

with variables and constants defined as above. For calculations, linear interpolations between the binary constituent values were used, with the exception of the piezoelectric constant.[25] The experimentally determined value of e_{14} from Ref. 33 was used for our calculations. To calculate confinement energies formally in the asymmetric well which includes the effects of the strain-induced field, numerical methods must be employed.[34] A rough approximation of the magnitude of the confined energy levels can be obtained using the semi-infinite triangular well model.[34,35] Although this approximation has limited applicability for shallow wells, we find that it provides us with an acceptable estimate of the confinement energies for several other samples. The presence of the strain-induced electric field allows the confined levels to shift deeper within the well according to the quantum-confined Stark Effect (QCSE). The intrinsic piezoelectric field present in the ⟨111⟩-grown system introduces an interesting complication to PL studies.[19–22,36] Upon excitation, the photogenerated electron-hole pairs are polarized by the strain induced piezoelectric field within the QW. The photoexcited carriers are polarized in such a way as to create a screening field, causing a decrease in the net field within the strained QW region.[10–13,37,38] The photogenerated carrier screening field causes a ''reversed'' QCSE resulting in an observed *blueshift* of optical transition energies. Researchers have used PL to confirm the existence of the internal fields by observing the related optical nonlinearities in the $In_xGa_{1-x}As$/GaAs material systems grown along the ⟨111⟩ direction.[7–9,15,18–22,39–41] The observed effect of the changes in the intrinsic field are consistent with those seen in PL studies of QW's under the influence of externally applied electric fields.[37] This optical nonlinearity is not observed in the ⟨100⟩-grown system.[42]

III. EXPERIMENTAL DETAILS

Our samples are $In_xGa_{1-x}As$/GaAs QW's grown using metal-organic chemical vapor deposition on ⟨100⟩ and ⟨111⟩A GaAs (slightly n-type) substrates. The latter were misoriented $\approx 2°$ toward the ⟨110⟩ axis. The two wells were grown simultaneously with nominal values of $x = 0.23$, well width of 24 ± 1 Å, and a GaAs cap layer of 550 Å. Details of sample growth and characterization have been published elsewhere.[43] The strained QW layer is well below the critical thickness for strain relaxation.[17] One important difference between ⟨111⟩- and ⟨100⟩-grown samples is the presence of the piezoelectric field in the ⟨111⟩-grown sample. This has been observed in lattice-matched systems of different growth directions.[44] For our study, thin wells (24 Å) were chosen for several reasons. The optical matrix element is less sensitive to small changes in electric field when compared with thicker wells.[22,40] We chose a single QW rather than a multiple-QW system, since study of a single, pseudomorphically strained QW layer has the advantage of isolation.[19–22,45] Coupling through thin barrier layers in MQW structures can play a significant role in carrier dynamics, particularly in the presence of an electric field.[46,47] Constraining the piezoelectric field to a single layer eliminates this complicated phenomenon. All PL measurements were taken with the sample sub-

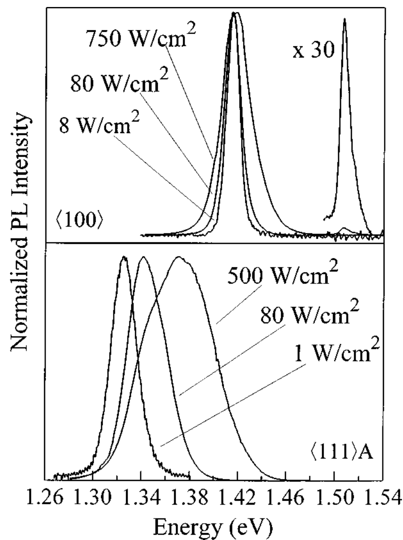

FIG. 1. Representative PL spectra of the two QW's studied at three different excitation intensities. Spectra have been normalized for comparison of position and line shape. Upper: $In_xGa_{1-x}As$/GaAs-⟨100⟩-grown single QW. Lower: $In_xGa_{1-x}As$/GaAs-⟨111⟩-grown single QW.

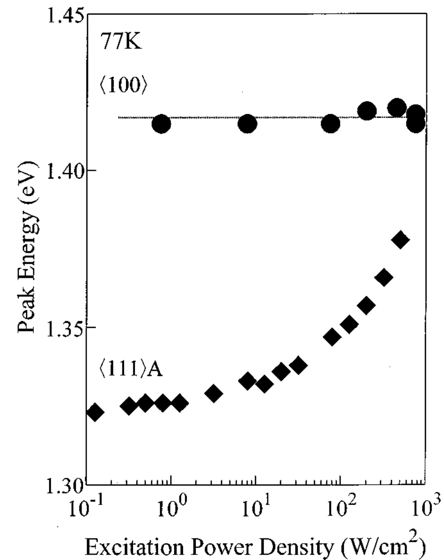

FIG. 2. Summary of peak energies for the ⟨100⟩-grown single QW and the ⟨111⟩-grown single QW.

mersed in liquid nitrogen (77 K). The 647.1-nm line of a Kr-ion laser was used as the PL excitation source. The 488.0-nm Ar-ion laser line was used to confirm our results. The PL signal was dispersed by a $\frac{1}{3}$-m single grating monochromator with slits set for instrumental resolution below 3 meV. The PL signal was detected with a liquid-nitrogen-cooled Ge detector, using an optical chopper and lock-in detection scheme. All spectra were corrected for the wavelength-dependent system response. Excitation intensity ($I_{\rm exc}$) studies were performed by using calibrated neutral density filters. Power densities range from 0.5–800 W/cm^2. The position and line shape of the GaAs band-gap emission (cap and substrate) were monitored over a wide range of $I_{\rm exc}$ in order to check for significant local heating effects. The maximum laser intensity was thereby kept sufficiently low to avoid local heating of the sample. Following measurements at high excitation intensity, we rechecked the spectrum at low excitation intensity to verify that the QW had suffered no damage by intense laser excitation.

IV. EFFECT OF EXCITATION INTENSITY ON PL SPECTRA

In Fig. 1 we show PL spectra of both the ⟨100⟩- and ⟨111⟩A-grown single QW's for range of excitation power densities, $I_{\rm exc}$. Spectra for the ⟨100⟩-grown QW show no significant energy shift over the 8–750 W/cm^2 excitation range studied. This confirms that no local heating occurs over this incident power density range, since local heating is accompanied by a redshift in peak energy. Peak position vs $I_{\rm exc}$ data are shown in Fig. 2. The peak energy observed at 1.420 eV compares well with our calculation of 1.423 eV for the ⟨100⟩ QW. We have not accounted for the exciton binding energy, which has been estimated to be ≈7 meV.[48] The large effect of confinement in the narrow QW is evident. The observed transition energy is large compared to the computed strained band-edge splitting of 1.250 eV. Our measured result is consistent with the HH1 confined level residing approximately midwell in the valence band and the $EC1$ level positioned very near the top of the conduction-band well. Confinement in this case adds over 150 meV to the band-edge energy splitting.

PL spectra for the ⟨111⟩-grown QW over a similar range of $I_{\rm exc}$ are shown in Fig. 1 (lower). These spectra clearly exhibit a large blueshift in the peak energy with increasing excitation intensity. The peak energy shifts from 1.322 to 1.378 eV for $I_{\rm exc}$ from 0.01 to 500 W/cm^2. Without accounting for the piezoelectric field, we calculate a band-edge splitting of 1.259 eV. We expect the confinement energies to be much smaller than those found for the ⟨100⟩ well, due to the large heavy-hole mass for [111] orientations.[49] Comparison of the observed energy of 1.322 eV (for $I_{\rm exc}<1$ W/cm^2) to the computed band-edge splitting confirms that the square well approximation is not valid for the ⟨111⟩A-grown well, since it yields large confinement energies (as found for the ⟨100⟩ QW case). Using the semi-infinite triangular well approximation and a field strength of ≈73 kV/cm from Eq. (6), we expect confinement energies of ≈38 meV (CB) and ≈23 meV (VB). This yields an expected transition energy of ≈1.320 eV. This simple approximation yields good agreement with the PL.

As illustrated by Fig. 2, over comparable ranges of $I_{\rm exc}$, the two emission energies of the QW's show vastly different behavior. For the ⟨100⟩ QW, the peak energy remains approximately constant. However, the ⟨111⟩ QW dramatically blueshifts. This verifies the existence of the piezoelectric field and its screening. However, we do not attribute the entire energy shift to piezoelectric field screening. We believe that the range of incident excitation intensities probes two regimes. In the lower range ($\lesssim 10$ W/cm^2) the observed blueshift in energy is due to piezoelectric field screening. Above this range, the large broadening toward higher energy of the emission is inconsistent with a single transition. Band-filling effects must also be considered, but cannot account for the large disparity between the PL from the ⟨100⟩ and ⟨111⟩-grown QW's at high intensities of photoexcitation. We

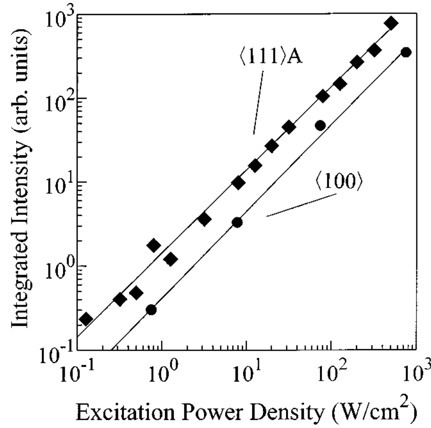

FIG. 3. Summary of excitation intensity dependence of the integrated PL intensity for the pair of QW's, along with results of least-squares fitting.

believe that the data may implicate the participation of higher lying levels, brought on by the complexities of the piezoelectric field present in the ⟨111⟩ QW. A quantitative examination of the linewidth and its dependence on excitation intensity given in Sec. VI provides the basis for this interpretation.

V. INTENSITY OF QW PL

The PL spectra were dominated by the QW emission even for the highest I_{exc}. Emission from the GaAs is observed for both QW's only for $I_{exc}>500\,W/cm^2$. The GaAs PL was difficult to observe, despite the fact that most of the photogenerated carriers are created in the GaAs. Carrier injection from the GaAs barrier layers into the well is the dominant process for producing free carriers in the well, particularly for thin wells and when the energy of excitation exceeds the energy gap of the barrier material.[50] Thus the dominance of the QW PL is expected, since the transfer rate between the barrier states and QW states is extremely fast.[36]

The observation that the QW's efficiently harvest carriers from the barriers is particularly true for the ⟨111⟩ system. In this case, QW PL persisted and was measurable for excitation power densities as low as $0.01\,W/cm^2$. This is in contrast to the ⟨100⟩-grown well luminescence, which was reliably observable only for excitation power densities one order of magnitude higher. Under the same experimental conditions, the integrated intensity of the ⟨111⟩ PL was greater by a factor of 2–3 than that seen for the ⟨100⟩-grown sample. This is interesting, since the presence of the piezoelectric field within the well layer results in a slightly reduced overlap integral of the confined envelope wave functions. The enhanced intensity of the ⟨111⟩-grown sample may be due to improved carrier capture, also a result of the presence of the piezoelectric field within the well.[51,44]

We now examine the dependence of the PL integrated intensity as a function of I_{exc}. Figure 3 shows a log-log plot of the data, along with least-squares linear fits. The PL intensity should have a power-law dependence on incident excitation intensity: $I_{PL}\propto I_{exc}^{\gamma}$.[52] We find $\gamma_{100}=1.03\pm0.05$ and $\gamma_{111}=0.98\pm0.06$. Both values are within experimental uncertainty of unity. This result is significant, since it may be taken as evidence of good interface quality. One effect of interface roughness is the creation of nonradiative recombination centers. These do not appear to play a dominant role in the recombination process for either the ⟨111⟩- or ⟨100⟩-grown sample. This result is remarkable for narrow wells, since interface roughness will have a pronounced effect in comparison to wider wells in which monolayer-scale roughness will be averaged out.

We also point out differences in the spectral line shapes between the ⟨100⟩ PL and that of the ⟨111⟩. At low excitation intensities, the line shapes are very similar and are consistent with band-band transitions between parabolic bands.[53] PL from the ⟨100⟩ QW exhibits broadening toward higher energy as excitation intensity is increased, but retains approximately the same line shape. This supports the fact that local heating is not a factor, since local heating generally causes a redshift, which we do not observe. In contrast, the ⟨111⟩ well acquires a more symmetric profile, tending toward a Gaussian line shape as I_{exc} is initially increased. At high excitation intensities ($I_{exc}>300\,W/cm^2$), the line shape appears inconsistent with a single transition, and indicates that higher-lying states may be involved in the observed PL emission. The CB well is expected to support only one confined electron level in the square-well approximation, relevant for the ⟨100⟩-grown QW. However, because confinement energies are evidently much smaller for the ⟨111⟩ QW, both the CB and VB may support a second confined level. Both these levels are expected to be very near the GaAs-barrier continuum energy levels. We attribute the large blueshift and broadening seen under high pump intensities primarily to the participation of either the CB or VB quasiconfined levels in the radiative emission. We rule out the participation of the $In_xGa_{1-x}As$ LH level since it should lie well below the top of the barrier VB edge for this system. This implies that the higher-energy emission stems from higher-lying levels in the conduction band.[21] This is discussed in more detail in Sec. VI.

VI. LINEWIDTH ANALYSIS

The ⟨111⟩ linewidth at low excitation intensity is $\approx 20\,meV$, only slightly wider than the ⟨100⟩ linewidth of $\approx 14\,meV$. The ⟨100⟩ PL linewidth is somewhat broader than reports of linewidths from other systems.[21] This may be due in part to the fact that our measurements are recorded at a higher temperature (77 K) than those of Ref. 21 (7 K). Additionally, fluctuations in layer thickness have a more pronounced effect for our thinner well samples, leading to larger linewidth values. The presence of the piezoelectric field in the ⟨111⟩ QW is expected to cause a slight broadening of the linewidth when compared with a similar ⟨100⟩-grown well. This is due to the piezoelectric field-induced spatial separation of the electronic and heavy-hole wave-function envelopes. The result is analogous to the effect of an external electric field on PL emission.[46]

The linewidth broadening with increased I_{exc} seen in the ⟨100⟩ PL is interpreted as follows. We find that the linewidth (Γ) data follow a power-law dependence of the form

$$\Gamma=\Gamma_o+\beta I_{exc}{}^{2/3}, \tag{7}$$

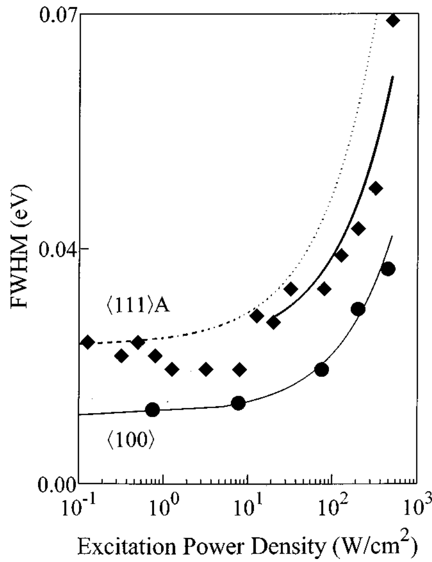

FIG. 4. Summary of linewidth (Γ) data for the ⟨100⟩- and ⟨111⟩-grown single QW's. Solid curves are from Eq. (6) over the ranges of validity as described in the text. The dashed curve is Eq. (6), illustrating poor agreement with the ⟨111⟩ QW PL data in the low I_{exc} range.

where Γ_o represents the limit of Γ at low excitation intensities. This function, with $\Gamma_o = 10 \pm 5$ meV and $\beta = (4 \pm 2) \times 10^{-4}$ as fit parameters,[54] is shown with the ⟨100⟩ PL data in Fig. 4. The exponent is consistent with the $\frac{2}{3}$ dependence of the position of the quasi-Fermi level on carrier density,

$$\epsilon_F^* = [(3\pi^2)^{2/3}\hbar^2/2m^*)]n^{2/3}, \tag{8}$$

where n is the photogenerated electron-hole pair concentration. This change in the position of the quasi-Fermi level assumes parabolic bands.[55] We approximate the number of photogenerated carriers[48]

$$n \approx (\alpha\tau/E_{\mathrm{exc}})I_{\mathrm{exc}}, \tag{9}$$

where $\alpha = 5.8 \times 10^4\,\mathrm{cm}^{-1}$ is the absorption coefficient[24] in the well and barrier materials, and $1/\tau$ is the recombination rate with $\tau \approx 1$ ns.[56] Using the reduced mass, and substituting Eqs. (7) and (8) into Eq. (6), we obtain reasonable agreement with the coefficient β.

Conceptually, I_{exc} is responsible for increasing n, filling the energy bands near the CB and VB edges. Competition between increasing excitation intensity and the natural bottleneck caused by the limited rate at which the QW can radiate, raise the quasi-Fermi level. The change in PL linewidth for the ⟨100⟩ QW is well described by carrier concentration-dependent band-filling effects. We refer to this as a dynamic Burstein-Moss effect. This scenario does not apply to the behavior of the ⟨111⟩ QW PL linewidth under high excitation conditions, as shown below.

We subsequently applied this analysis to the ⟨111⟩ linewidth, fixing $\Gamma_o = 20$ eV. The agreement is poor, as is evident from the dashed line on the ⟨111⟩ linewidth data in Fig. 4. This implies that the change in linewidth for the ⟨111⟩ system cannot be explained solely in terms of band filling. Band-filling effects in no way account for the very slight *decrease* we observe in linewidth in the 0.01 to $\approx 12\,\mathrm{W/cm}^2$ excitation intensity range. We associate the diminishing linewidth in this low excitation intensity range to screening of the piezoelectric field. This results in greater envelope-function overlap which reduces the emission linewidth.

Since a blueshift due only to piezoelectric field screening is accompanied by a corresponding *decrease* in linewidth,[56] we use the linewidth data to estimate the value of I_{exc} at which the screening becomes complete and band filling begins to dominate. This value is $I_{\mathrm{exc}} \approx 15\,\mathrm{W/cm}^2$. Over the 0.01–15-W/cm^2 excitation intensity range, we observe the peak energy to blueshift by ≈ 0.016 eV. If we assume that the strain-induced electric field is uniform over the width of the thin QW, the magnitude of the field can be roughly approximated as $F_{\mathrm{pz}} = \Delta E/L \approx 70\,\mathrm{kV/cm}$, where we take L as the nominal well width. This is in good agreement with the value of 73 kV, found above using Eq. (6). We would also point out that, in systems which exhibit a piezoelectric field, determination of the PL peak position and linewidth must be done with great care. Variations in excitation intensity can shift the line position and even diminish the linewidth.

Our ability to reach the flatband condition is consistent with the identification of the system as mechanically clamped.[7–9] However, when the number of photogenerated carriers exceeds that required for complete field screening (flatband condition), we must consider other mechanisms for the blueshift in energy with increasing optical excitation intensity above $\approx 12\,\mathrm{W/cm}^2$ in Fig. 4. Because the photogenerated carriers cannot drive the bands *beyond* the flatband condition (i.e., cause a reversal in the net field direction), further increase in carrier densities results in the onset of bleaching and possibly the participation of higher-lying transitions.[7–9] This is in agreement with straightforward calculations of the energy levels using the semi-infinite, triangular-well approximation.

We confirmed that consideration of simple band filling is inadequate in this case by using the analysis for the linewidth data from our ⟨100⟩ well for the corresponding data from the ⟨111⟩-oriented sample in the range $I_{\mathrm{exc}} > 12\,\mathrm{W/cm}^2$. This result is shown as the solid line on the ⟨111⟩ linewidth data in Fig. 4. The agreement is good only for mid-range I_{exc}. We attribute the poor agreement at high I_{exc} primarily to the onset of emission by higher lying transitions, suggested by the spectral line shape in Fig. 1. The emission appears to be composed of several bands in the high excitation intensity range. Plausible assignments for the higher-lying transition include near-continuum states in the CB of the well to the HHVB level. Additionally, a type-II emission from the GaAs barrier CB level to the well HHVB state is possible. The close proximity of the CB levels in the well and barrier is in agreement with our hydrostatic pressure work.[26] This result calls attention to the very different behavior of the ⟨111⟩ PL under variations in I_{exc} when compared to the ⟨100⟩ PL. This dramatic difference is not surprising, since the carrier dynamics at high excitation rates are very different in the two wells. Once the ⟨111⟩ QW has reached the flatband regime, the well is highly excited and saturated with carriers, allowing for the participation of higher-lying, quasibound, conduction-band levels which are not present in the ⟨100⟩ system. This is in contrast with the situation in the ⟨100⟩

QW, where the emission is seen to be consistent with a single emission, even at the highest attempted excitation intensity.

VII. SUMMARY

We have used excitation dependent photoluminescence spectroscopy to examine differences in the photoluminescence spectrum of a simultaneously grown pair of $In_xGa_{1-x}As$ narrow single QW's with different crystal growth axes. We find striking differences in the power density dependence of the peak energy, line shapes, and of the PL spectra for the two wells. In contrast, both wells exhibit a linear dependence on incident power density for the PL integrated intensity. The linewidth of the ⟨100⟩ PL is accurately modeled by band-filling effects as I_{exc} is increased, while PL emission from the ⟨111⟩ well cannot be explained by the simple model. By careful analysis of the excitation intensity dependence of the ⟨111⟩ linewidth the point at which the flatband condition (complete screening of the QW internal field) is determined. This allows us to estimate experimentally the strain-induced piezoelectric field of 70 kV/cm. For I_{exc} in excess of the full-screening value, band-filling effects cannot adequately explain the evolution of the PL shape, which dramatically broadens toward higher energy. This marked difference between the behavior of the ⟨111⟩ and ⟨100⟩ PL under high excitation intensity conditions may be attributed to the participation of higher-lying CB levels in the ⟨111⟩ QW. However further studies of this interesting system are necessary to fully understand the origin of the PL in the ⟨111⟩-grown system under high excitation intensities. The PL from the ⟨111⟩ QW was observable for extremely low incident power densities, approximately an order of magnitude lower than the point at which the PL from the ⟨100⟩ system became unobservable.

ACKNOWLEDGMENTS

The authors wish to thank T. S. Moise for a careful reading of this manuscript. T.S. gratefully acknowledges the National Science Foundation for support of this work.

*Deceased.

[1] L. J. Mawst, A. Bhattacharya, M. Nesnidal, J. Lopez, D. Botex, and J. A. Morris, Appl. Phys. Lett. **67**, 2901 (1995).

[2] Makoto Kudo and Tomoyoshi Mishima, J. Appl. Phys. **78**, 1685 (1995).

[3] J. W. Matthews and A. E. Blakeslee, J. Cryst. Growth **27**, 118 (1974).

[4] Fred H. Pollak, in *Strained-Layer Superlattices*, edited by Thomas P. Pearsall Semiconductors and Semimetals Vol. 32 (Academic, San Diego, 1990), Chap. 2.

[5] I. J. Fritz, P. L. Gourley, and L. R. Dawson, Appl. Phys. Lett. **51**, 1004 (1987).

[6] R. People and S. A. Jackson, in *Strained-Layer Superlattices* (Ref. 4), Chap. 2.

[7] X. R. Huang, D. R. Harken, A. N. Cartwright, D. S. McCallum, Arthur L. Smirl, J. L. Sánchez-Rojas, A. Sacedón, F. González-Sanz, E. Calleja, and E. Muñoz, J. Appl. Phys. **76**, 7870 (1994).

[8] X. R. Huang, D. S. McCallum, D. R. Harken, A. N. Cartwright, and Arthur L. Smirl, Superlattices Microstruct. **15**, 171 (1994).

[9] X. R. Huang, D. R. Harken, A. N. Cartwright, Arthur L. Smirl, J. L. Sánchez-Rojas, A. Sacedón, E. Calleja, and E. Muñoz, Appl. Phys. Lett. **67**, 950 (1995).

[10] D. L. Smith, Solid State Commun. **57**, 919 (1986).

[11] D. L. Smith and C. Mailhiot, J. Vac. Sci. Technol. A **5**, 2060 (1987).

[12] D. L. Smith and C. Mailhiot, Phys. Rev. Lett. **58**, 1264 (1987).

[13] D. L. Smith and C. Mailhiot, Rev. Mod. Phys. **62**, 173 (1990).

[14] Walter G. Cady, *Piezoelectricity* (McGraw-Hill, New York, 1946).

[15] K. W. Goossen, E. A. Caridi, T. Y. Chang, J. B. Stark, D. A. B Miller, and R. A. Morgan, Appl. Phys. Lett. **56**, 715 (1990).

[16] D. Gershoni, J. M. Vandenberg, S. N. G. Chu, H. Temkin, T. Tanbun-Ek, and R. A. Logan, Phys. Rev. B **40**, 10 017 (1989).

[17] T. G. Andersson, Z. G. Chen, V. D. Kulakovskii, A. Uddin, and J. T. Vallin, Appl. Phys. Lett. **51**, 752 (1987).

[18] B. K. Laurich, K. Elcess, C. G. Fonstad, J. G Beery, C. Mailhiot, and D. L. Smith, Phys. Rev. Lett. **62**, 649 (1989).

[19] T. S. Moise, L. J. Guido, J. C. Beggy, S. Sestadie, and R. C. Barker, J. Electron. Mater. **21**, 119 (1992).

[20] T. S. Moise, L. J. Guido, R. C. Barker, J. O. White, and A. R. Kost, Appl. Phys. Lett. **60**, 2637 (1992).

[21] T. S. Moise, J. L. Guido, and R. C. Barker, Phys. Rev. B **47**, 6758 (1993).

[22] T. S. Moise, J. L. Guido, and R. C. Barker, J. Appl. Phys. **74**, 4681 (1993).

[23] T. G. Andersson, Z. G. Chen, V. D. Kulakovskii, A. Uddin, and J. T. Vallin, Phys. Rev. B **37**, 4032 (1988).

[24] Shun Lien Chuang, *Physics of Optoelectronic Devices*, edited by J. Goodman (Wiley, New York, 1995).

[25] *Strained-Layer Superlattices*, edited by O. Madelung (Springer-Verlag, Berlin, 1991).

[26] T. Sauncy, M. Holtz, O. Brafman, D. Fekete, and Y. Finkelstein, following paper, Phys. Rev. B **59**, 5056 (1999).

[27] R. A. Hogg, T. A. Fisher, A. R. K. Willcox, D. M. Whittaker, M. S. Skolnick, D. J. Mowbray, J. P. R. David, A. S. Pabla, G. J. Rees, R. Grey, J. Woodhead, J. L. Sanchez-Rojas, G. Hill, M. A. Pate, and P. N. Robson, Phys. Rev. B **48**, 8491 (1993).

[28] Gerald Bastard, *Wave Mechanics Applied to Semiconductor Heterostructures* (Les Editions de Physique, Paris, 1988).

[29] Richard L. Tober and Thomas B. Bahder, Appl. Phys. Lett. **63**, 2369 (1993).

[30] Thomas B. Bahder, Richard L. Tober, and John D. Bruno, Phys. Rev. B **50**, 2731 (1994).

[31] Thomas B. Bahder, Phys. Rev. B **51**, 10 892 (1995).

[32] V. Swaminathan and A. T. Macrander, *Materials Aspects of GaAs and InP Based Structures* (Prentice-Hall, Englewood Cliffs, NJ, 1991).

[33] J. L. Sánchez-Rojas (private communication).

[34] R. André, C. Deshayes, J. Cibert, L. S. Dang, S. Tatarenko, and K. Saminadayar, Phys. Rev. B **42**, 11 392 (1990).

[35] Claude Weisbuch and Borge Vinter, *Quantum Semiconductor Structures: Fundamentals and Applications* (Academic, New York, 1991).

[36] A. Chtanov, T. Baars, and M. Gal, Phys. Rev. B **53**, 4704 (1996).

[37] S. Fafard, E. Fortin, and J. L. Merz, Phys. Rev. B **48**, 11 062 (1993).
[38] D. R. Harken, X. R. Huang, D. S. McCallum, and Arthur L. Smirl, Appl. Phys. Lett. **66**, 857 (1995).
[39] Y. Matsui and Y. Kusumi, J. Appl. Phys. **78**, 7137 (1995).
[40] P. J. Rodríguez-Gironés and G. J. Rees, IEEE Photonics Technol. Lett. **7**, 71 (1995).
[41] E. Vanelle, A. Alexandrou, J.-P. Likforman, D. Block, J. Cibert, and R. Romestain, Phys. Rev. B **53**, R16 172 (1996).
[42] P. Boring, B. Gil, and U. J. Moore, Phys. Rev. Lett. **71**, 1875 (1993).
[43] Y. Finkelstein, E. Zolotoyabko, M. Blumina, and D. Fekete, J. Appl. Phys. **79**, 1869 (1996).
[44] T. Hayakawa, T. Suyama, M Kondo, M. Hosada, S. Yamamoto, and Y. Hijikata, J. Appl. Phys. **64**, 2764 (1988).
[45] N. G. Anderson, W. D. Laidig, R. M. Kolbas, and Y. C. Lo, J. Appl. Phys. **60**, 2361 (1986).
[46] G. Bastard, E. E. Mendez, L. L. Chang, and L. Esaki, Phys. Rev. B **28**, 3241 (1983).
[47] R. Grey, J. P. R. David, P. A. Claxton, F. Gonzalez Sanz, and J. Woodhead, J. Appl. Phys. **66**, 975 (1989).
[48] P. J. Harshman and S. Wang, J. Appl. Phys. **71**, 5531 (1992).
[49] Kenichi Nishi and Takayoghi Anan, J. Appl. Phys. **70**, 5004 (1991).
[50] Z. S. Piao, H. I. Jeon, S. S. Cha, K. Y. Lim, E.-K. Suh, and H. J. Lee, Appl. Phys. Lett. **65**, 333 (1994).
[51] X. Chen, C. H. Molloy, D. A. Woolf, C. Cooper, D. J. Somerford, P. Blood, K. A. Shore, and J. Sarma, Appl. Phys. Lett. **67**, 1393 (1995).
[52] M. V. Karachevtseva, A. S. Ignat'ev, V. G. Mokerov, G. Z. Nemtsev, V. A. Strakhov, and N. G. Yaremenko, Semiconductors **28**, 691 (1994).
[53] Peter Y. Yu and Manuel Cardona, *Fundamentals of Semiconductors: Physics and Material Properties* (Springer-Verlag, New York, 1996).
[54] The units of β are $kg^{1/3}\,m^2$ when the analysis is carried out in MKS units. The coefficient we determine reflects corrections necessary for power densities in W/cm^2.
[55] Jian De-Sheng, Y Makita, K. Ploog, and H. J. Queisser, J. Appl. Phys. **53**, 999 (1982).
[56] A. N. Cartwright, D. S. McCallum, Thomas F. Boggess, Arthur L. Smirl, T. S. Moise, L. J. Guido, R. C. Barker, and B. S. Wherrett, J. Appl. Phys. **73**, 7767 (1993).